Absence of backscattering in the quantum Hall effect in multiprobe conductors

M. Büttiker
IBM Thomas J. Watson Research Center, P.O. Box 218, Yorktown Heights, New York 10598
(Received 21 March 1988)

Under certain conditions, high magnetic fields in a two-dimensional conductor lead to a suppression of both elastic and inelastic backscattering. This, together with the formation of edge states, is used to develop a picture of the integer quantum Hall effect in open multiprobe conductors. We consider both ideal contacts without elastic scattering and also disordered contacts. Ideal contacts populate edge states equally whereas disordered contacts lead to an initial nonequilibrium population of the edge states. In Hall samples much larger than an inelastic length, and in the presence of disordered contacts, the sample edges become equipotential lines only an inelastic scattering length away from the current source and current drain contacts. Samples so small that the carriers can travel from one contact to the other without inelastic relaxation do not exhibit exact quantization if the contacts are disordered. In all cases we find that the quantum Hall effect occurs only if the sample exhibits at least two sets of equilibrated edge states which do not interact via elastic or inelastic scattering. The onset of interaction between the two sets of edge states leads to deviations from exact quantization and eventually to a breakdown of the quantum Hall effect.

I. INTRODUCTION

The discovery of the integer quantum Hall effect by von Klitzing, Dorda, and Pepper[1] has spurned a considerable effort to understand this phenomenon.[2] An elegant explanation of this effect was put forth by Laughlin.[3] Laughlin discusses the response of a cylinder to an Aharonov-Bohm flux along the axis of the cylinder and explains the quantum Hall effect in terms of a supercurrent due to the long-range phase rigidity of the wave functions around the loop. Halperin[4] supplemented this picture by discussing edge states which form at the boundary of the sample. The long-range phase rigidity has led Imry[5] to propose several flux-sensitive effects. We do not question these papers, but point out that the rigidity of wave functions is not necessary for the existence of Hall currents. Arguments which invoke phase-rigid wave functions, sensitive to an Aharonov-Bohm flux, are, however, limited to conductors for which the distance a carrier has to travel to enclose the flux is short compared to an inelastic-scattering length.[6] Clearly, typical experimental samples, in which the quantum Hall effect is measured, are many orders of magnitude larger than the inelastic-scattering length. Moreover, experiments are performed on open conductors with contacts as shown in Fig. 1 and not the closed conductors which are the subject of Refs. 3 and 4. Therefore, it is desirable to supplement the discussions of Laughlin and Halperin with arguments which lead to the quantum Hall effect even in large open conductors, where we can not expect phase coherence along the entire length of the sample. The need to establish a closer relationship between these basic theoretical arguments which apply to special geometries and the experimental arrangements was also pointed out by Niu and Thouless.[7]

The explanation leading to the quantum Hall effect put forth in this paper is based on the suppression of backscattering in high magnetic fields: Carriers moving along the edge of the sample in a high magnetic field cannot effectively reverse direction if scattered at an impurity or by an inelastic event. Carriers scattered at an impurity are, at best, reflected backwards a distance determined by the diameter of a cyclotron orbit. Under the action of the driving force provided by the confining potential, the carriers will continue to move along the edge of the sample. This picture is correct as long as the impurity potential varies smoothly over a cyclotron radius, but rapidly compared to the sample dimensions. It is also correct if the impurity potential is strong but of short range and the mean distance between impurities exceeds a cyclotron radius. Similarly, the inelastic length must exceed the magnetic length. This has the consequence that edge states continue to provide current-carrying channels despite elastic and inelastic scattering.

Experimentally, what is measured are resistances in a four-terminal configuration: Two of the contacts, k and l, of the sample in Fig. 1 are used to feed and draw current, and two contacts, m and n, are used to measure the voltage difference. The measured resistances obey the

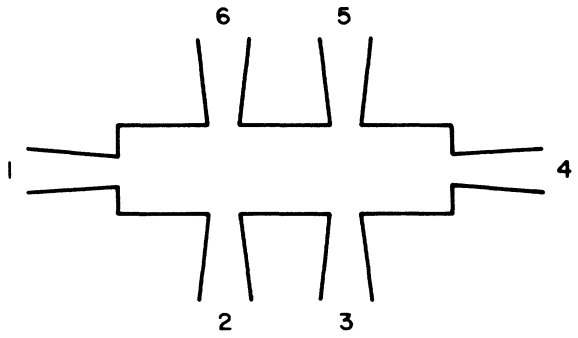

FIG. 1. Conductor with Hall bar geometry.

reciprocity theorem,[8]

$$\mathcal{R}_{kl,mn}(\mathbf{B})=\mathcal{R}_{mn,kl}(-\mathbf{B}) . \quad (1.1)$$

The resistance measured in a particular configuration of current contacts k,l and voltage contacts m,n in the presence of a field $\mathbf{B}$ is the same as the resistance measured if the field $\mathbf{B}$ is reversed and the current and voltage contacts are exchanged. The reciprocity theorem is closely related to the Onsager-Casimir symmetry relation for the (global) conductances[8-11] (not the symmetry of the local conductivity tensor). For samples without macroscopic inhomogeneities, the quantum Hall effect can be considered to be the following phenomena: Imagine a line in the interior of the sample which connects the current-source and current-sink contacts k and l. Then the quantum Hall effect is characterized by a resistance $\mathcal{R}_{kl,mn}=h/e^2N$ for all the pairs of voltage contacts m,n with one member of the pair on each side of the line introduced above. Simultaneously, the resistances for pairs of voltage probes with both members of the pair on the same side of this line vanish. The resistances which characterize the quantum Hall effect are four-probe resistances and the voltage contacts are distinct from the current-drain contacts. A *satisfactory* explanation of the quantum Hall effect has to demonstrate that the four-probe resistances take these particular values *even* under circumstances where the three-terminal resistances $\mathcal{R}_{kl,km}$ (one voltage measurement is made at the current-source terminal) and the two-terminal resistances $\mathcal{R}_{kl,kl}$ (the voltage measurements are made at the current source and drain) are not quantized (or zero.)

In open conductors contacts play a crucial role: We show that a contact acting as a current source populates the states of the sample, the edge states, with a nonequilibrium distribution. Only under ideal conditions can we expect that the initial population of all the edge states, on one side of the sample, is the same. The initial population of the quantum states hinges on the properties of the contacts. Thus, typically, the edge states become populated equally only an *inelastic*-scattering length away from a current contact. Our investigation shows that exact quantization of the Hall resistance occurs only if the Hall probes are at least an inelastic length away from the current source and current drain. This suggests that inelastic scattering plays an important role in establishing exact quantization of the Hall resistance.

Both the contacts connecting the sample to the current drain and current source and the contacts connecting the sample to voltmeters are of importance. At low magnetic fields voltage probes are dissipative.[12,13] Despite the fact that no net current flows into a voltage probe, the energy flux between the sample and the voltmeter is, in general, not zero.[13] Thus, a voltage contact, by its very presence, can cause an additional potential drop along the sample. However, in the quantum Hall effect this cannot be the case. We show that the sample edge can become an equipotential line regardless of the number of voltage contacts. Again, we find that it is the peculiar nature of scattering in high magnetic fields which explains the nondissipative nature of voltage probes in the quantum Hall effect. We find that the voltage probes are nondissipative, but, nevertheless, introduce incoherence into the conduction process. This is possible since a voltage probe in the quantum Hall effect is in perfect equilibrium with the sample edge.

While one of our goals is to address the quantum Hall effect in macroscopic multiprobe samples, there have appeared a number of both experimental[14-18] and theoretical[19-24] papers addressing properties of the Hall effect in small conductors. Since inelastic scattering plays an important role in establishing the quantum Hall effect in macroscopic samples, it is interesting to ask what happens to the Hall effect in open conductors so small that a carrier can traverse the conductor from one contact to the other without suffering inelastic events. We investigate four-probe phase-coherent conductors. We find, indeed, that exact quantization does not occur if two or more adjacent contacts are disordered. A contact is termed disordered if a carrier in the conductor approaching the contact leaves the conductor with a probability less than 1.

Discussions of the quantum Hall effect, typically, investigate the response of the current to an applied external field. A "longitudinal" field cannot exist in the steady state since it causes carriers to pile up at one edge of the sample and depletes the other edge. Evidently, the quantum Hall effect is characterized by the fact that over a large portion of the sample edges become equipotential lines. Hence, the total electric field component parallel to the sample edge has to be zero. Therefore, often, the current is calculated in response to a "transverse" external field.[25] This has the consequence that current flows in the bulk of the sample in contrast to the discussion given below which leads to carrier flow only along the edges of the sample. Calculations which do not treat the electric field self-consistently have only a limited predictive value and might, in fact, be misleading. To circumvent the problems associated with this approach, it has been proposed that we apply a longitudinal field for a limited time only in order to induce current flow.[26] This is possible in closed conductors, but does not help to understand the quantum Hall effect in the open conductor of Fig. 1.

It is therefore useful to approach the quantum Hall effect from a different point of view. Instead of taking the external field as the causative agent, we follow Landauer[27,28] and view the currents as the driving forces. The electric field can be obtained by calculating the charges which pile up as a consequence of carrier flow. More precisely, we specify the *incident* carrier flux as a function of the chemical *potential of all the terminals.* The net current is then calculated and, via probabilities for reflection at the sample and transmission through the sample, is related to the chemical potentials of the terminals. Using the wave functions at the Fermi energy, a self-consistent solution of the electrical potential must be found which matches at the contacts the value of the chemical potential. This approach has been implemented in Ref. 8, in which a multiprobe resistance formula is derived, and this is discussed in Ref. 10 in more detail. In Refs. 8 and 10 it is stressed that it is the Fermi level of a contact which is measured at a voltage probe. It is this latter property of this particular implementation of the

Landauer approach which leads to Eq. (1.1) and thus to resistances which are compatible with the (global) Onsager-Casimir symmetry relations. An earlier approach[29] defined resistance with regard to local electric potentials in the perfect portions of the conductor away from the terminals. There is no fundamental reason that requires a resistance defined by invoking local electric potentials to exhibit a particular symmetry. Indeed, as shown in Ref. 10, this earlier formulation does not lead to the reciprocity-symmetry equation (1.1). Experiments on ultrasmall metallic lines,[30] on macroscopic conductors of various geometries,[31] and on quantum Hall samples[32] all exhibit reciprocity symmetry. Therefore, it is clearly necessary to use a formulation which leads to resistances which are compatible with these fundamental symmetries.

A discussion of the quantum Hall effect, invoking Ref. 29 (local potentials away from terminals), has been given by Streda *et al.*[19] Jain and Kievelson[20,21] apply the one-channel Landauer formula.[27,28] These papers study local electric potentials in a two-terminal conductor. As in Ref. 29, the piled-up charges are determined in the perfect portions of the conductor to the left and right of a disordered region only. The role of contacts is not addressed. In these papers[19–21] the longitudinal resistance vanishes only if the two-terminal conductance is also quantized. The authors of Refs. 19 and 20 obtain a "sum rule" for the Hall resistance and the longitudinal resistance, which is appropriate for three-terminal resistances.[10] In experiments, as pointed out already, the Hall resistance and the longitudinal resistances are four-terminal resistances. Four-terminal resistances obey a more complex sum rule.[8,10] Despite our criticism of the work of Streda *et al.*,[19] we emphasize its pioneering character. Reference 19 has provided a large portion of the motivation for this paper. Beenakker and van Houten[22] and Peeters[24] have pointed to the applicability of the four-terminal formula of Ref. 8 to the quantum Hall effect and the work presented here proceeds in the same direction.

II. THE TWO-TERMINAL CONDUCTANCE

A. Ideal perfect conductor

Consider an ideal two-dimensional conductor without impurities or inhomogeneities of width w connecting two electron reservoirs as shown in Fig. 2(a). The electron reservoirs at chemical potentials μ_1 and μ_2 serve as source and sink of carriers and of energy. A reservoir emits carriers into current-carrying states up to its chemical potential. Every carrier reaching a reservoir, independent of phase and of energy, is absorbed.

Let us first briefly consider the case of zero magnetic field. The Hamiltonian of the perfect conductor is

$$H=\frac{1}{2m}(p_x^2+p_y^2)+V(y) \ . \tag{2.1}$$

Here, x is the coordinate along the strip and y is the coordinate transverse to the strip. The wave functions are separable and of the form

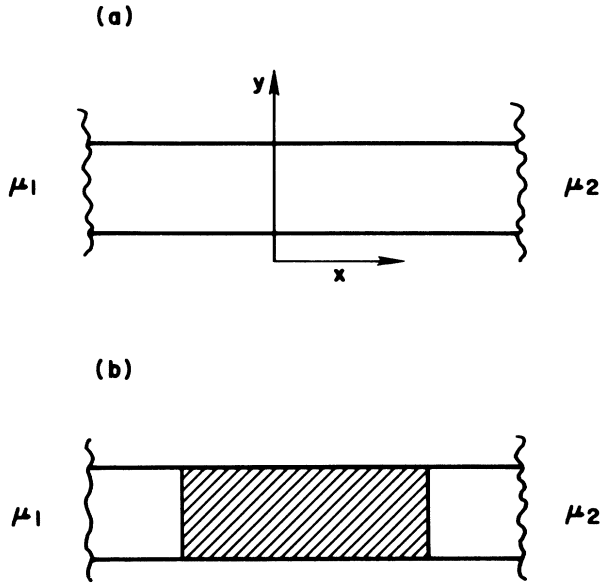

FIG. 2. (a) Perfect two-dimensional conductor connected to reservoirs. The chemical potentials of the reservoirs are μ_1 and μ_2. (b) Conductor with a disordered region (shaded part) connected to the left and right to perfect conductors which, in turn, connect to reservoirs.

$$\psi_{j,k}(x,y)=e^{ikx}f_j(y) \ . \tag{2.2}$$

k is the wave vector along x, and $f_j(y)$ is a transverse eigenfunction with energy eigenvalue E_j. The total energy of the state is the sum of the transverse energy E_j and the energy for longitudinal motion. Thus at the Fermi energy $E_F=E_j+\hbar^2k_j^2/2m$, there are $2N$ states, where N is the number of transverse energies E_j below the Fermi energy. Let us calculate the current through this perfect conductor assuming $\mu_1>\mu_2$. Below μ_2 left- and right-moving states are equally occupied, and the net current is zero. Thus we need to be concerned only with the energy interval between μ_2 and μ_1. The current injected by the left reservoir in channel j is $I_j=ev_j(dn/dE)_j\Delta\mu$. Here, $v_j=\hbar^{-1}(dE_j/dk)$ is the longitudinal velocity at the Fermi energy of channel j. $(dn/dE)_j$ is the density of states at the Fermi energy for this channel and $\Delta\mu=\mu_1-\mu_2$. In one dimension the density of states is $dn/dk=1/2\pi$ and hence $(dn/dE)_j=1/2\pi\hbar v_j$. Therefore, the current fed into a channel is

$$I_j=(e/h)\Delta\mu \ , \tag{2.3}$$

independent of the channel index j. The total current is $I=N(e/h)\Delta\mu$. Here, as in the remaining part of the paper, we assume that kT is small compared to the separation of the transverse energy levels. The voltage drop between the reservoirs is $eV=\Delta\mu$. Thus the two-terminal resistance of a perfect N-channel wire is

$$\mathcal{R}=\frac{h}{e^2}\frac{1}{N} \ . \tag{2.4}$$

This result depends on the way current is fed from the reservoir into the perfect conductor. Later, we shall con-

sider more realistic contacts and discuss how that changes Eq. (2.4). For the remainder of this section we continue to use this simple model of current-feeding and current-drawing contacts.

Next, consider the perfect conductor in a magnetic field. We take the vector potential $\mathbf{A}=(-By,0,0)$. The Hamiltonian is

$$H=\frac{1}{2m}\left[\left[p_x-\frac{e}{c}By\right]^2+p_y^2\right]+V(y)\ . \tag{2.5}$$

The magnetic field induces cyclotron motion of the carriers. The wave function is still separable and of the form $\psi_{j,k}=e^{ikx}f_j(y)$. This leads to an eigenvalue problem for the function f,

$$Ef=\left[-\frac{\hbar^2}{2m}\frac{\partial^2}{\partial y^2}+\frac{m}{2}\omega_c^2(y_0-y)^2+V(y)\right]f\ . \tag{2.6}$$

Here, $\omega_c=|eB|/mc$ is the cyclotron frequency and m the effective mass. In addition, the eigenvalues of Eq. (2.6) depend on the parameter

$$y_0=-\frac{\hbar k}{m}\frac{1}{\omega_c}=-kl_B^2\ , \tag{2.7}$$

where $l_B=(\hbar c/|eB|)^{1/2}$ is the magnetic length. Consider a range of y for which the confining potential is constant. We take $V(y)\equiv 0$. The solutions of Eq. (2.6) are harmonic-oscillator wave functions with a width proportional to the magnetic length l_B with eigenvalues

$$E_{jk}=\hbar\omega_c(j+\tfrac{1}{2})\ , \tag{2.8}$$

where $j=0,1,2,\ldots$; Eq. (2.8) is independent of the parameter y_0 (i.e., independent of k). This picture must change near the edges of the sample at y_1 and y_2. The cyclotron motion is affected by the confining potential.[4,33] Classically, the carriers perform motion along skipping orbits. As a function of y_0 the eigenvalues depart from the Landau formula, Eq. (2.8), and increase as the edge is approached, as shown in Fig. 3. For a hard-wall potential, near the edges, the energy of a state depends on the center y_0 through the distance y_1-y_0 to the lower edge and y_2-y_0 to the upper edge. In general, the energy of a state is determined by[4,33]

$$E_{jk}=E(j,\omega_c,y_0(k))\ . \tag{2.9}$$

Using arguments similar to those applied to Bloch functions, one can show that carriers in an edge state acquire a longitudinal velocity,

$$v_{jk}=\hbar^{-1}\frac{dE_{jk}}{dk}=\hbar^{-1}\frac{dE_{jk}}{dy_0}\frac{dy_0}{dk}\ , \tag{2.10}$$

which is proportional to the slope of the Landau level. dE/dy_0 is negative at the upper edge y_2 and positive at the lower edge y_1 (see Fig. 3). In a strong magnetic field pointing out of the page, dy_0/dk is negative and, therefore, the velocity along the upper edge is positive and negative along the lower edge. Note that it is only the edge states which can contribute to carrier flow because the bulk Landau states (the region in Fig. 3, where E is

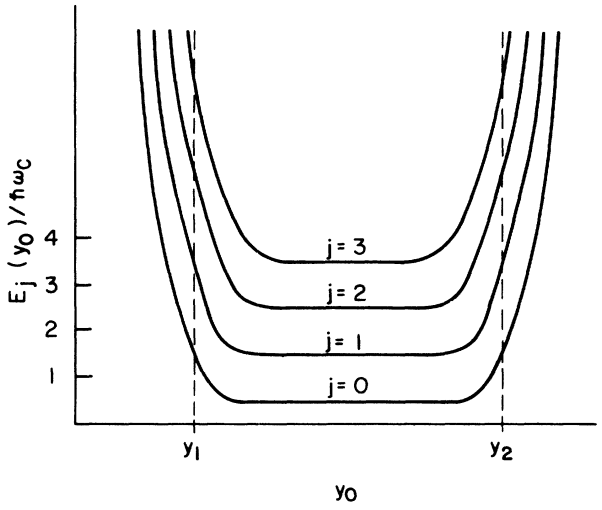

FIG. 3. Energy spectrum of a perfect conductor in a high magnetic field for a rectangular confining potential (walls at y_1 and y_2). The Landau levels at $E_j=\hbar\omega_c(j+\frac{1}{2})$ are strongly bent upwards near the edges of the sample. y_0 is the center of the harmonic-oscillator wave functions. After Ref. 4.

independent of y_0) have no velocity. The magnetic field quenches the kinetic energy for longitudinal motion. The density of states along a Landau level E_j can also be found from $dn/dk=1/2\pi$ appropriate for one-dimensional conductors. Since $dn/dk=(dn/dy_0)|dy_0/dk|$, we find, using Eq. (2.7), that $dn/dy_0=2\pi l_B^2$. Away from the edges, the density of states is determined by a dense packing of cyclotron orbits in the plane. Further, the density of states is related to the velocity as in the conductor at zero field,

$$\left[\frac{dn}{dE}\right]_j=\frac{dn}{dk}\left[\frac{dk}{dE}\right]_j=\frac{1}{2\pi\hbar v_{jk}}\ .$$

The states at the Fermi energy are determined by the equation $E_F=E_{jk}$, with E_{jk} given by Eq. (2.9). This equation determines the values of k at the Fermi energy, $k_n(E_F)$. There is a discrete number $n=1,\ldots,N$ of states (N with positive k and N with negative k). As the Fermi energy changes and passes through a bulk Landau energy, the number of edge states intercepting the Fermi energy drops discontinuously from N to $N-1$. The current fed into each edge state is

$$I=ev_j\left[\frac{dn}{dE}\right]_j(\mu_1-\mu_2)=\frac{e}{h}\Delta\mu\ .$$

Thus, the current fed into an edge state by a reservoir is the same as the current fed into a quantum channel in a zero-field perfect conductor. The resulting two-terminal resistance for a perfect conductor in a high magnetic field is thus

$$\mathcal{R}=\frac{h}{e^2}\frac{1}{N}\ . \tag{2.11}$$

Here, N is the number of edge states (with positive veloci-

ty). Equations (2.4) and (2.11) are two-terminal resistances and not Hall resistances. Neither Eq. (2.4) nor Eq. (2.11) remains unaffected by elastic scattering, as will be discussed below.

Consider what happens with increasing magnetic field. From exactly solvable models, for instance, for a quadratic confinement potential, we know that the magnetic field increases the transverse energies $E_j(B) > E_j(0)$. Thus the number of current-carrying states N is a function of the magnetic field. With increasing magnetic field there are fewer quantum channels (edge states) below the Fermi energy. The conductance drops by e^2/h as a channel rises above the Fermi level. This has recently been observed in experiments by van Wees *et al.* and by Thornton *et al.*[34]

Equations (2.4) and (2.11) are not fundamental; they describe a very idealized situation where there is no scattering both along the perfect conductor and in the way current is fed into the conductor and leaves the conductor. Before these results are applied to a physical situation,[34] the discussion has to be expanded to include the scattering events which cause a departure from the ideal situation treated here. We discuss modifications of the ideal situations in the following sections of this paper.

Let us discuss the origin of the resistances (2.4) and (2.11) in some more detail. Why do the perfect conductors exhibit a resistance at all? Separately, Imry,[35] Büttiker,[13] and Landauer[28] have pointed to the phenomena of contact resistances.[36,37] A brief and semiclassical discussion has been given by Sharvin.[36] In the reservoirs the carriers are distributed according to an equilibrium Fermi function. As the carriers enter the perfect conductor, a redistribution of the population of states with positive and negative velocity must be achieved such that the states with positive velocity are occupied to a higher energy then the states with negative velocity. Such a redistribution has to occur since we have a net flow of carriers in the perfect conductor. Thus the two-terminal resistance, Eqs. (2.4) and (2.11), are contact resistances.

As emphasized already, these contact resistances are sensitive to the disorder configuration of the sample and the geometry of the contact.[28,10] We do not expect contact resistances to be universal, i.e., independent of geometry and disorder. Below, we show that there is no fundamental link between these contact resistances and the quantum Hall effect. A sample, with equipotential lines along the edges, is completely characterized by contact resistances. However, the contact resistances need not be quantized. Before addressing this we continue the discussion of the two-terminal conductor.

B. Conductor with elastic scattering

The conductor in Fig. 2(b) exhibits a disordered section, connected at its left and right ends to ideal perfect conductors.[27–29] The disordered part of the conductor mixes the channels of the perfect conductors. Carriers incident in channel j (edge state j) from the left have probability amplitude t_{ij} for transmission into channel i and probability amplitude r_{ij} for reflection into channel i. The corresponding probabilities for carriers incident from the right are denoted with a prime. More specifically, the wave function describing carriers incident in channel j from the left is in the left-hand perfect conductor given by

$$\psi_j(x,y) = \sum_{i=1}^{i=N} [\delta_{ij} e^{ik_i x} + (v_j/v_i)^{1/2} r_{ij} e^{-k_i x}] f_i(y) , \quad (2.12)$$

and in the right-hand perfect conductor by

$$\psi_j(x,y) = \sum_{i=1}^{i=N} (v_j/v_i)^{1/2} t_{ij} e^{-ik_i x} f_i(y) . \quad (2.13)$$

In the disordered region, ψ_j is a complicated function of x and y. The current incident in channel j is given by Eq. (2.3). The fraction of this current which is transmitted is

$$I = \frac{e}{h} \sum_{i=1}^{i=N} T_{ij} \Delta\mu ,$$

where $T_{ij} = |t_{ij}|^2$. Here, we have assumed that the energy dependence of T_{ij} can be neglected in the small energy range from μ_2 to μ_1. Summing over all incident channels gives a total transmitted current

$$I = \frac{e}{h} \sum_{i=1,\, j=1}^{i=N\, j=N} T_{ij} \Delta\mu .$$

The voltage drop is $eV = \Delta\mu$, and we thus find a Landauer resistance,

$$\mathcal{R} = \frac{h}{e^2} \frac{1}{T} , \quad (2.14)$$

where $T = \sum_{i=1,\, j=1}^{i=N,\, j=N} T_{ij}$ is the total transmission probability through the disordered region. Microreversibility implies that the total transmission probability is a symmetric function of the magnetic field.[10] Let us stress that Eq. (2.14) is valid in the presence of an arbitrary magnetic field. The validity of Eq. (2.14) rests only on a well-defined scattering problem, but is independent of the particular nature of the channels. Whether we deal with zero-field quantum channels,[29,38] Landau states, or Bloch states is immaterial. However, since the chemical potentials of the reservoirs are related to the current via Eq. (2.14), a self-consistent electric potential $eU(x,y)$ which obeys the boundary condition[10] $eU(x,y) \to \mu_1$ to the left and $eU(x,y) \to \mu_2$ to the right does not, in general, exist if the number of quantum channels N in the reservoirs is not much larger than $h/e^2\mathcal{R}$. We return to this point below.

At low magnetic fields elastic scattering at an impurity leads to transmitted waves and reflected waves in all the channels, if the impurity and the sample do not have a particular symmetry. If the disordered region contains many impurities, such symmetries are certain to be absent. Thus at low fields elastic scattering completely mixes the channels and is bound to produce deviations from Eq. (2.4). What happens as we increase the magnetic field? Let us now investigate elastic scattering due to disorder in the presence of a high magnetic field. Figure 4 depicts a single impurity near the edge of a sample. The quasiclassical skipping orbits are scattered by this impurity, but due to the magnetic field the scattered or-

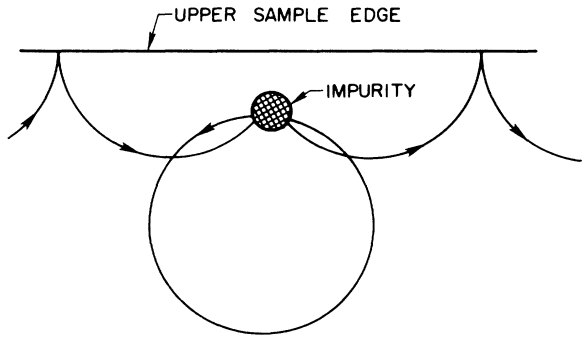

FIG. 4. Quasiclassical skipping orbits along the upper edge of the sample in presence of a localized impurity. In a high magnetic field backscattering over distances large compared to the cyclotron radius is suppressed.

bits are never further then a cyclotron radius away from the edge. After scattering (possibly a number of times) by the impurity, the orbits return to the edge and continue to follow the edge. Computations of wave functions in disordered samples do show edge states which extend only a small distance away from the sample boundary.[39] If we consider a box larger than a cyclotron radius enclosing this impurity, we see that every carrier that enters this box arriving in one of the edge states will leave this box traveling *forward* in one of the edge states. The key point is that an impurity cannot effectively reverse the direction of motion of a carrier. *There is no scattering backwards against the flow of carriers over distances which are large compared to the cyclotron radius.* Even in the presence of many impurities in the shaded part of Fig. 2(b), backscattering is suppressed as long as the mean distance between impurities is large compared to the cyclotron radius. It is this property, the suppression of backscattering in the presence of a high magnetic field, which gives rise to the quantum Hall effect. The scattering matrix describing transmission through the box (see Fig. 5) must have the property that the transmission from all the edge states into the edge state i,

$$T_i = \sum_{j=1}^{N} T_{ij} \ , \tag{2.15}$$

is equal to 1. It is not necessary that each edge state remains immune to elastic scattering (i.e., that[19] $T_{ij}=\delta_{ij}$). Scattering from one edge state to another is permitted as long as the scattering occurs among edge states on the same side of the sample. The same consideration for impurities along the lower edge leads to the conclusion that

$$T_i' = \sum_{j=1}^{j=N} T_{ij}' \tag{2.16}$$

is equal to 1. Here, the prime denotes transmission probabilities for carriers incident from the right. Thus carriers incident in a particular edge state will, as a consequence of impurity scattering, emerge in other edge states. However, the transmission probabilities are such that, if all the incident edge states are full up to a chemical potential μ, then all the outgoing edge states are also full up to the same chemical potential. At low fields elastic scattering typically mixes all the channels. In high magnetic fields elastic scattering mixes only the channels of the upper edge and mixes the channels of the lower edge (see Fig. 5). Only states with either positive velocity (upper edge) or negative velocity (lower edge) are mixed.

From the quasiclassical considerations [Fig. 2(b)] we can expect that the carriers cannot be scattered from one edge of the sample to the other as long as the cyclotron radius is small compared to the mean distance between impurities. Denote the distance between impurities by l_e. To obtain a criterion for the strength of the field, we can make use of the fact that the Landau states are harmonic-oscillator wave functions. The spatial width of a state in the jth Landau level is

$$(\langle \Delta y^2 \rangle)^{1/2} = l_B (j+\tfrac{1}{2})^{1/2} \ . \tag{2.17}$$

In a narrow wire, scattering at impurities will not provide a path from the upper edge to the lower edge as long as the width of the states is small compared to the mean distance between impurities, l_e. This yields a lower critical field $B_{\rm crit}$ for the onset of backscattering. For $B > B_{\rm crit}$ the two-terminal resistance is given by Eq. (2.11). For $B < B_{\rm crit}$ the two-terminal resistance is not quantized, but given by Eq. (2.14). Comparison of Eq. (2.17) with the elastic length yields a critical field $B_{\rm crit}$ for the observation of N steps, $2\pi l_e^2 B_{\rm crit} > \Phi_0(N+\frac{1}{2})$. The flux through a circle with radius given by the mean distance between impurities must exceed $N+\frac{1}{2}$ single-charge flux quanta $\Phi_0 = hc/e$. Similarly, for narrow ballistic wires of width w, the criterion for the suppression of backscattering is $2\pi w^2 B_{\rm crit} > \Phi_0(N+\frac{1}{2})$. In GaAs the mean elastic length is of the order of up to 10 000 Å, whereas narrow wires can be fabricated with a width roughly 10 times smaller.

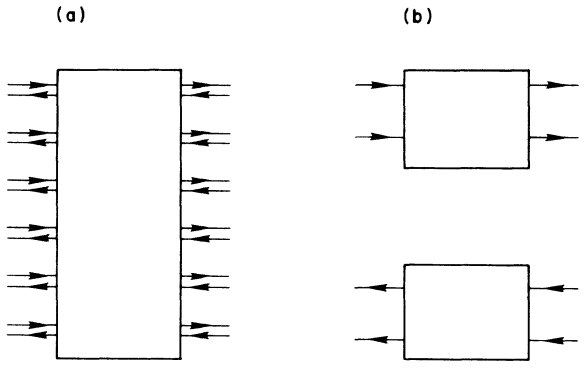

FIG. 5. Symbolic representation of the scattering properties at (a) small magnetic fields and (b) high magnetic fields. The arrows on the box represent the incoming and outcoming quantum channels in the perfect wires adjacent to the disordered region in Fig. 2(b). A flux incident in one channel gives rise to outgoing waves in all the channels at low magnetic fields. At high magnetic fields an incoming flux along the upper edge from the left gives rise to outgoing currents only to the right along the upper edge. The scattering matrix can be divided into two portions, each of which is reflectionless, one for the upper edge states and one for the lower edge states.

Thus, compared to a relatively pure sample a narrow wire can be more restrictive for the onset of backscattering. Experiments by Roukes *et al.*[17] show a suppression of the low-field Hall effect in narrow wires, proportional to $w^{-3/2}$. In addition, the experiments also indicate that the Hall effect is not antisymmetric at low fields.[8,30] Theoretical work by Beenaker and van Houten[22] explains the quenching of the Hall effect by analyzing the transverse extension of the edge states. A detailed explanation of these experiments also needs to take the dependence of the confining potential on the wire width into account.[40] In addition, as we discuss below, the Hall effect and its properties near breakdown do depend on the properties of the contacts.

The suppression of backscattering for dilute impurity concentrations is easy to understand. Interestingly, in wide enough samples backscattering can be suppressed even in the limit of a high impurity concentration, i.e., when the cyclotron radius is large compared to the mean distance between impurities. This interesting result was first obtained from the scaling theory of two-dimensional electron conduction in high magnetic fields.[41] As explained by Laughlin,[42] with increasing impurity concentration the bulk Landau levels rise in energy. This floating of the bulk Landau levels permits extended states in the center of the Landau band and localized states between the Landau levels even in the presence of a high impurity concentration. The quasiclassical argument discussed above cannot be applied to this case because the interference effects of multiple-scattering events are neglected. In the dilute-impurity-concentration limit backscattering is suppressed over a distance large compared to the cyclotron radius. In contrast in the high-concentration limit backscattering is suppressed only over distances large compared to the localization length, which, in turn, is large compared to a cyclotron radius.

The absence of backscattering is decisive for the appearance of the quantum Hall plateaus. This can be seen in the following way: The voltage $U(x,y)$ in the conductor of Fig. 2(b) in the limit of strong screening (see the Appendix for a derivation and discussion of this result) and low magnetic fields is given by[10,43]

$$eU(x,y)=\frac{\sum_{i=1}^{i=N}\frac{1}{v_i}[\,|\psi_i(x,y)|^2\mu_1+|\psi_i'(x,y)|^2\mu_2]}{\sum_{i=1}^{i=N}\frac{1}{v_i}[\,|\psi_i(x,y)|^2+|\psi_i'(x,y)|^2]}\,. \tag{2.18}$$

Typically, all the wave functions contribute. If, on the other hand, backscattering is suppressed, and the wave functions describing carriers incident from the left remain confined to the upper edge and the wave functions describing carriers incident from the right (prime) remain confined to the lower edge, we obtain near the upper edge (index u)

$$eU_u=eU(x,y_2)=\frac{\sum_{i=1}^{i=N}\frac{1}{v_i}|\psi_i(x,y_2)|^2\mu_1}{\sum_{i=1}^{i=N}\frac{1}{v_i}|\psi_i(x,y_2)|^2}=\mu_1\,. \tag{2.19}$$

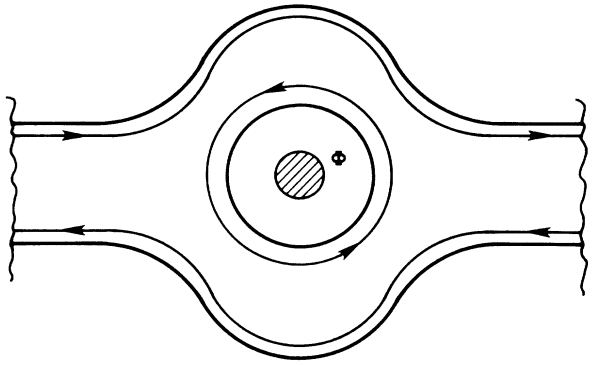

FIG. 6. Open quantum Hall conductor with a hole penetrated by an Aharonov-Bohm flux. The fine lines indicate the current-carrying states.

Similarly, for the lower edge (index 1), we find $eU_1=eU(x,y_1)=\mu_2$. Thus the upper and lower edges are equipotential lines.

Using $T_i=1$ and $T_i'=1$ we find a current $I=(e/h)N(\mu_1-\mu_2)$. The Hall voltage is $U_u-U_1=\mu_1-\mu_2$, and the Hall resistance is thus $\mathcal{R}=(h/e^2)(1/N)$. However, note that the solution $eU_u=\mu_1$ and $eU_1=\mu_2$ independent of x is not compatible with our boundary condition. $eU(x,y)$ has to be identical to μ_1 in the left-hand reservoir and has to be identical to μ_2 in the right-hand reservoir. To satisfy these boundary conditions, we must describe the contacts more carefully.

Let us next briefly discuss the states in the bulk of the sample. Consideration of the quasiclassical orbits in the presence of an isolated impurity shows that they give rise to circulating-current paths. For a single impurity (dilute limit) the current path is within a cyclotron radius of the impurity. An example of a circulating-current path is evident in the geometry of Fig. 6, where a hole has been introduced into the conductor. In the Aharonov-Bohm geometry a set of edge states develops along the hole of the conductor. For the outer edges of the sample to remain equipotential lines, the inner edge states must be disconnected from the outer ones. Elastic scattering is not permitted to transfer carriers from the inner edge

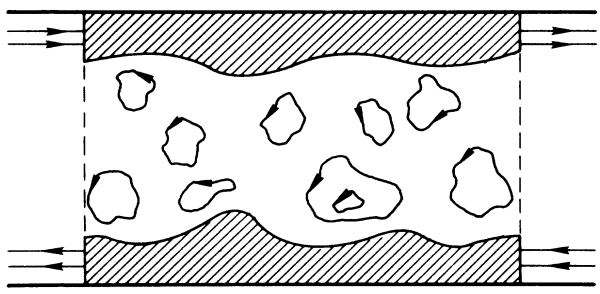

FIG. 7. Current-carrying states in the conductor of Fig. 2(b) with the Fermi level equal or near a bulk Landau level for a potential which fluctuates slowly compared to the magnetic length, but fast compared to the width of the sample. Away from the edge states (shaded) in the bulk the current-carrying states form loops.

states to the outer edge states. If that is the case, it is easy to see that the two-terminal conductance is not sensitive to the flux through the hole of the conductor, i.e., there is no Aharonov-Bohm effect. For the wave functions to be sensitive to the flux through the hole, they must enclose the flux. The outer edge states, which determine the conductance through the sample, do not do that. In order to observe an Aharonov-Bohm effect, scattering from the inner edge states to the outer edge states must be permitted.[21] That, however, is accompanied by a potential drop along the outer edges of the sample. (In the metallic Aharonov-Bohm effect the hc/e oscillations[6,30,44] persist to very high fields because carrier motion is diffusive.) Therefore, the reason that the h/e oscillations in the experments of Ref. 16 decrease with increasing field and eventually vanish is a direct consequence of the suppression of backscattering in high magnetic fields.

Instead of a hole through the conductor as in Fig. 6, consider a smoothly varying potential[45] with fluctuations small compared to $\hbar\omega_c$. Such a potential disturbs the bulk Landau states of the perfect conductor and gives rise to circular current-carrying states as shown qualitatively in Fig. 7. With perfect leads attached to the disordered region of the sample [compare Fig. 2(b)], the current-carrying states in the bulk are necessarily circular: current enters and leaves the sample only through edge states. Backscattering is suppressed for Fermi energies for which there are no current paths connecting the upper and lower edges.

C. Conductor with inelastic scattering

The reservoirs connected to the perfect conductors in Fig. 2 serve not only as a source and sink of carriers but also of energy. For a simple description of the effect of inelastic events, we can therefore also invoke reservoirs as a means to randomize the phase of the wave function.[12,13] We divide the sample into regions over which motion of carriers is coherent and separate these regions by reservoirs. Samples which are many inelastic lengths long can be built up in this way. Figure 8(a) shows a conductor of length $L=Ml_{\rm in}$ divided into M coherent regions of length $l_{\rm in}$. The total resistance of this conductor is obtained by summing the resistances of each segment using Eq. (2.12). Since the phase is totally randomized between segments, the resistances add classically. Let T_i denote the total transmission probability through the ith segment. The resistance of the conductor is

$$\mathcal{R}=\left[\frac{h}{e^2}\right]\sum_{i=1}^{i=M}\frac{1}{T_i}\ , \tag{2.20}$$

where T_i is the *total* transmission probability of the ith coherent region. Equation (2.20) can be used to discuss the Thouless approach[46] to one-dimensional localization.[13]

In the presence of a high magnetic field, Fig. 8(a), and Eq. (2.20), do not apply. Inelastic backscattering is also suppressed by the magnetic field. For $l_{\rm in}>l_c$ carriers in the upper edge states cannot be scattered into the lower edge states. Thus, the division of the sample into

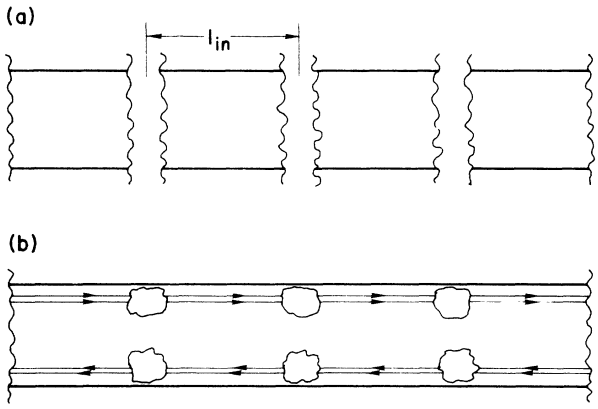

FIG. 8. Inelastic scattering in conductors long compared to an inelastic-scattering length. Inelastic scattering is represented by phase-randomizing reservoirs. (a) At low fields these reservoirs connect to all quantum channels. (b) At high fields, when the Fermi level is in a gap between bulk Landau levels, the reservoirs disrupt the phase of the upper and lower edge states separately.

coherent regions, separated by phase-randomizing reservoirs, must look as in Fig. 8(b). Each bath acts only on one set of edge states. Since there are only incoming states to one side of such a reservoir and only outgoing states on the other side of the reservoir, there is no drop in chemical potential associated with the reservoirs in Fig. 8(b). The upper and lower edges of the sample remain equipotential lines. This is a crucial point, and we return to it in the next section. The two-terminal resistance is $\mathcal{R}=(h/e^2)(1/N)$, independent of the length of the sample.

Let us now discuss inelastic scattering for the case that the Fermi energy is close to the center of a Landau level. In Fig. 7 we have depicted the circulating-current paths in the bulk of the sample. In the absence of inelastic scattering, these states do not contribute to current transport through the sample. Conduction is along edge states only. However, if we permit inelastic scattering, transitions from one of the current loops to the next can occur. Since the states describing circular currents are at slightly different energies, hopping from one loop to the other has to be activated. Thus for energies near the center of a Landau level, we can expect an activated contribution to the conductance. (Clearly, the edge states at this energy also contribute to the conductance.) In the case that no elastic scattering from the upper edge to the lower edge occurs, it is only the inelastic contribution to the conductance which leads to a rounding of the quantum Hall steps.

D. Disordered contacts

So far, we have assumed that a reservoir supplies carriers to edge states up to the chemical potential of the reservoir. Thus the edge states are filled completely. That is strictly correct only if the transition from the reservoir into perfect conductors occurs without elastic scattering. In many problems the exact nature of the boundary conditions is not of primary importance. In

the quantum Hall effect we are, however, interested in the conditions under which the sample edges become equipotential lines. In the discussion given above, the upper edge is, under quantum Hall conditions, an equipotential $eU_u=\mu_1$, where μ_1 is determined by the reservoir to the left. The lower edge is an equipotential line eU_1 determined by the reservoir to the right, $eU_1=\mu_2$. This picture has to be revised for two reasons: First, as pointed out already, a self-consistent solution $eU(x,y)$ must match the potentials of the reservoirs to the left and right. Hence, the sample edges cannot be equipotential lines along the whole conductor. Second, elastic scattering at the connection of the conductor to the reservoir can lead to a nonequilibrium population of the edge states.

Let us investigate a situation where current is fed into the edge states through a disordered region. Scattering at the contacts is characterized by total transmission probabilities T_1, T_2 and by total reflection probabilities R_1, R_2 in the following way: Consider the left-hand-side contact in Fig. 9. To the right of the disordered region, conditions, are such that edge states are possible. At the contact the two-dimensional electron gas is connected to a wire in which three-dimensional motion is allowed. Thus at the terminal two-dimensional Landau quantization is not effective. We have a large number of states at the Fermi energy; a large number of available states is what characterizes a reservoir. For the purpose of this paper, the precise nature of the states in the reservoir, their sensitivity to the magnetic field, does not matter. In order to describe the transition from the conductor to the reservoir with a scattering matrix, we assume to the left of the disordered region again a perfect conductor with a large number of states at the Fermi energy. Assume now that it is the states to the left which are filled up to the chemical potential μ_1. Each of these states has a transmission probability $T_{ij}(\mathbf{B})$ for transmission into a Landau edge state to the right. Let the number of edge states be N and the number of states in the contact be M. The current fed into the ith Landau level is

$$I=\frac{e}{h}\sum_{j=1}^{M} T_{ij}(\mu_1-\mu_2) .$$

If $\sum_j T_{ij}<1$, the edge is only partially filled, between μ_2 and μ_1. The total current fed into the N edge states is $I=(e/h)T(\mu_1-\mu_2)$, where the total transmission probability of the contact is

$$T=\sum_{i=1}^{N}\sum_{j=1}^{M} T_{ij} .$$

Note, that differing edge states are filled to a different degree,

$$\sum_j T_{ij}\neq\sum_j T_{kj} .$$

From now on we consider only contacts with a large density of states M. Such contacts can still behave in an ideal fashion. If every carrier incident from an edge on the contact leaves the sample, we have $T=N$. Since $M\ll N$, most carriers incident from the reservoir on the two-dimensional region are scattered back into the reservoir. It is only the carriers incident from the two-dimensional region which have probability 1 of reaching the reservoir. An ideal contact is characterized by the absence of "internal" reflection, but exhibits "external" reflection. A contact which is not ideal, i.e., a contact with $T<N$, will be called "disordered." A fraction of the carriers incident from the lower (upper) edge states on a disordered contact skips along the contact and reaches the upper (lower) edge states. A disordered contact exhibits both internal and external reflection.

As carriers move past a disordered contact into the sample into the edge states, inelastic scattering becomes effective and starts to equilibrate the populations of the edge states with each other. Inelastic scattering is represented in Fig. 9 by reservoirs at a potential μ_A along the upper edge. As we have seen by analyzing the conductor of Fig. 8(b), the edge states, once they have been equilibrated, remain in equilibrium. Similarly, in the presence of disordered contacts the lower sample edge is not at the chemical potential of the current drain, but at a somewhat elevated chemical potential μ_B.

Let us calculate the potentials μ_A and μ_B. The total transmission probability (if all M incident channels are full) of the left-hand-side disordered contact is denoted T_1. The total probability for carriers incident in the lower edge states for reflection into the upper edge states is denoted R_1. The total probability for transmission and reflections for carriers incident from the left are denoted T_1' and R_1'. Current conservation and microreversibility requires $T_1'=T_1$, $N=R_1+T_1$, and $M=R_1'+T_1$. Similarly, the probability for transmission through the right-hand-side contact for carriers incident along the upper edge is denoted T_2, and the probability for reflection of these carriers into the lower edge states is R_2. With these specifications we can calculate the currents I_1 between the contact and the first reservoir at potential μ_A and the current I_2 between the right-hand-side contact and the first reservoir at the chemical potential μ_B. Relative to the chemical potential μ_2 of the current drain, the current I_1 has two contributions: carriers incident through the contact give a contribution $(e/h)T_1(\mu_1-\mu_2)$. Along the lower edge a current $(e/h)N(\mu_B-\mu_2)$ is incident on the contact. A fraction $(e/h)R_1(\mu_B-\mu_2)$ is reflected into the upper edge states. Thus the current along the upper edge states is

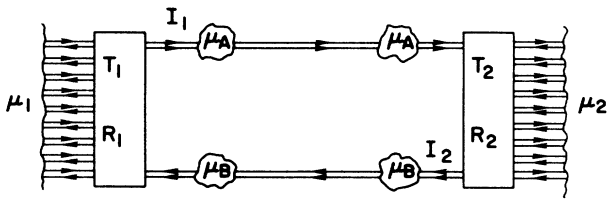

FIG. 9. Conductor with disordered contacts which lead to an initial nonequilibrium population of the edge states. Reservoirs at chemical potentials μ_A and μ_B disrupt the phase of the edge states.

$$I_1=(e/h)T_1(\mu_1-\mu_2)+(e/h)R_1(\mu_B-\mu_2)\ . \tag{2.21}$$

The first reservoir equilibrates the differing population of the edge states. The current leaving this reservoir is $(e/h)N(\mu_A-\mu_2)$. Thus the chemical potential μ_A is determined by

$$I_1=(e/h)N(\mu_A-\mu_2)\ . \tag{2.22}$$

This current is incident on the right-hand side contact, and the portion of the current which is reflected to the lower edge states is

$$I_2=(e/h)R_2(\mu_A-\mu_2)\ . \tag{2.23}$$

An inelastic-scattering length away from the contact, this current is equilibrated. Thus the chemical potential μ_B is determined by

$$I_2=(e/h)N(\mu_B-\mu_2)\ . \tag{2.24}$$

Equations (2.21)–(2.24), with a little algebra, give the chemical potentials

$$\mu_A=\mu_2+\left[\frac{NT_1}{N^2-R_1R_2}\right](\mu_1-\mu_2)\ , \tag{2.25}$$

$$\mu_B=\mu_2+\left[\frac{T_1R_2}{N^2-R_1R_2}\right](\mu_1-\mu_2)\ , \tag{2.26}$$

and the total current from source to drain,

$$I=(e/h)T_2(\mu_A-\mu_2)$$
$$=\frac{NT_1T_2}{N^2-R_1R_2}(\mu_1-\mu_2)\ . \tag{2.27}$$

The two-terminal resistance differs from the ideal value given by Eq. (2.11) and is given by

$$\mathcal{R}=e(\mu_1-\mu_2)/I=\left[\frac{h}{e^2}\right]\frac{N^2-R_1R_2}{NT_1T_2}\ . \tag{2.28}$$

An inelastic length away from the current source and the current drain the edges of the sample are, however, equipotential lines and the difference in chemical potentials, the Hall voltage, is given by

$$eU_H=\mu_A-\mu_B=\frac{NT_1T_2}{N^2-R_1R_2}(\mu_1-\mu_2)\ . \tag{2.29}$$

The Hall resistance is found to be

$$\mathcal{R}_H=eU_H/I=(h/e^2)(1/N)\ . \tag{2.30}$$

These considerations clearly show the stability of the quantum Hall effect with regard to nonideal contacts and further highlight that inelastic scattering, which leads to an equilibrium of the edge states, plays a role in establishing exact quantization. To establish the quantum Hall effect in macroscopic conductors, we only need to convince ourselves that the probes, used to measure the potential difference between the upper and lower edges of the sample, do not change the picture developed here either.

The current induced by the difference in chemical potentials $\Delta\mu=\mu_1-\mu_2$ in the conductor of Fig. 9 consists of two contributions: there is a direct current $I-I_2$ along the upper edge of the sample and a circular current I_2 following the sample edges. I_2, which is also proportional to $\Delta\mu$, can thus be viewed as a diamagnetic current induced by the applied potential difference. In Ref. 47 the same phenomenon, in metallic submicron conductors at low fields, is discussed, where circular patterns can occur on a length scale small compared to the inelastic length. *In contrast diamagnetic currents in high fields, in the absence of backscattering, occur over macroscopic length scales and do not require rigidity of the phase of the wave function.*

III. THE QUANTUM HALL EFFECT IN MACROSCOPIC SAMPLES

Figure 10 shows a Hall bar sample with six contacts. The contacts are separated by a distance exceedings the inelastic-scattering length such that, in our symbolic representation of inelastic scattering, there is at least one phase-randomizing reservoir along the edge connecting two contacts. Suppose contact 1 and contact 4 are the current source and current drain. Let us now show that the chemical potentials of the phase-randomizing reservoirs are given by μ_A and μ_B and are given by Eqs. (2.25) and (2.26) with T_2 and R_2 replaced by T_4 and R_4. To show this, it is sufficient to demonstrate that a voltage contact does not lead to a potential drop along the edge, i.e., the voltage contacts measure the chemical potentials of the phase-randomizing reservoirs. Voltage probes equilibrate with the sample and there is, therefore, no net current flow between the sample and the voltage contact. Consider probe 6 at a chemical potential μ_6. The carrier flux from the sample edge at chemical potential μ_A toward the voltage contact is $N(\mu_A-\mu_2)/h$. The fraction of flux leaving the sample is $T_6(\mu_A-\mu_2)/h$. On the other hand, the voltage contact injects a flux $T_6(\mu_6-\mu_2)/h$ into the sample into the edge states leading away from the contact. Equating these two fluxes yields the measured chemical potential $\mu_6=\mu_A$. Thus the chemical po-

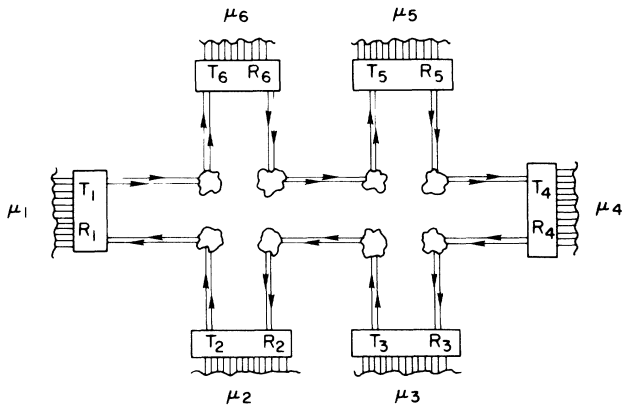

FIG. 10. Macroscopic sample with Hall bar geometry and disordered contacts. The resistive behavior of the sample in a Hall plateau is determined by contact resistances characterized by transmission and reflection probabilities. Coherent carrier motion from one contact to the other is prevented by phase-randomizing reservoirs.

tential of the measurement probe is the same as that of the phase-randomizing reservoirs. Moreover, in addition to the flux $T_6(\mu_A-\mu_2)/h$ injected by the measurement probe into the sample, the flux incident on the contact and reflected at the contact $R_6(\mu_A-\mu_2)/h$ adds to give a total flux $N(\mu_A-\mu_2)/h$. Thus the edge states leading away from the probe are populated equally and the same way as the edge states leading up to the voltage contact. Therefore, the voltage probes in Fig. 10 do change the geometry of the equipotential lines, but leave the value of the potential unaffected. We emphasize that this dissipation free behavior of contacts is special to the quantum Hall effect.

With contact 1 and contact 4 as current and voltage source, the resistances $\mathcal{R}_{14,65}$ and $\mathcal{R}_{14,23}$ are zero, and the resistances $\mathcal{R}_{14,62}=\mathcal{R}_{14,53}=\mathcal{R}_{14,63}$ are quantized and given by Eq. (2.30). Clearly, for the conductor of Fig. 10, we could choose any pair of probes as current sources and current contacts with results that are equivalent to those just discussed.

Next, we return to the subject of contact resistances. Let us keep contact 1 and contact 4 as current source and current drain. There are four contact resistances which can be determined. If the voltage difference between the current source and contact 6 is measured, we obtain

$$\mathcal{R}_{14,16}=(\mu_1-\mu_6)/eI=(h/e^2)(R_1/NT_1)\ . \tag{3.1}$$

Here, we have taken into account that $\mu_6=\mu_A$ is given by Eq. (2.25) and the current I by Eq. (2.27) with T_2 and R_2 replaced by T_4 and R_4. If probe 2 is used to measure the potential difference to μ_1, we obtain

$$\mathcal{R}_{14,12}=(\mu_1-\mu_2)/eI=(h/e^2)(1/T_1)\ . \tag{3.2}$$

Similarly, for the contact resistances of contact 4, we obtain

$$\mathcal{R}_{14,54}=(\mu_5-\mu_4)/eI=(h/e^2)(1/T_4) \tag{3.3}$$

and

$$\mathcal{R}_{14,34}=(\mu_3-\mu_4)/eI=(h/e^2)(R_4/NT_4)\ . \tag{3.4}$$

Experiments[48] indicate that the two-terminal resistance differs typically not very much from the Hall resistance. (For specially prepared contacts, quantization of the two-terminal resistance of better than 1 part in 10^{-8} has been measured.) Such contacts which exhibit almost no internal reflection have to be described by total transmission probabilities close to N. The resistance given by Eq. (3.1) is then close to zero, whereas the contact resistance given by Eq. (3.2) is close to the quantized Hall resistance. Thus the potential along the upper edge of the sample drops slightly as we move along the edge away from the current source, stays constant along most of the edge, and starts to drop strongly as the current sink is approached. Along the lower edge, the situation is reversed. Most of the drop of the potential occurs close to the current source, and a much smaller drop occurs as the current sink is approached. Since most of the current is carried along the upper edge the carriers lose most of the energy $\mu_1-\mu_2$ near the current sink. It would be interesting to perform an experiment to see if this prediction is correct. A heat-sensitive device near contact 4 should reveal the production of Joule heat for one polarity of the field, but should be close to the ambient temperature if the field is reversed.

The four resistances given by Eqs. (3.1)–(3.4) contain four unknown transmission and reflection coefficients. By measuring these resistances the unknown probabilities T_i and R_i can be expressed in terms of the measured contact resistances. Once the T_i and R_i are known, all the possible resistance measurements on the conductor of Fig. 10 can be predicted. For fields B in a plateau region, *the resistive behavior of the sample is completely determined by its contact resistances.*

The discussion given above applies only if the contacts are separated by more than an inelastic-scattering length. There is at least one phase-randomizing reservoir disrupting the phase of the edge states connecting two probes in the conductor of Fig. 10. Since, for disordered contacts, inelastic scattering plays a crucial role in establishing the quantum Hall effects, the question arises whether small multiprobe conductors do indeed exhibit a quantum Hall effect. It is this question which we want to address in the next section of the paper.

IV. QUANTUM HALL EFFECT IN PHASE-COHERENT CONDUCTORS

To investigate the role of contacts in the quantum Hall effect in small samples, we start by considering the conductor shown in Fig. 11. We assume that transmission through the conductor is elastic. Inelastic events occur only in the reservoir. Thus in the conductor of Fig. 11 phase-coherent transport from one contact to the other is possible. The relation between the chemical potentials of the contacts and the currents at the contacts (positive if carrier flow is from the bath to the conductor) is given by[8,10]

$$I_i=(e/h)\left[(N_i-R_i)\mu_i-\sum_{j\neq i}T_{ij}\mu_j\right]\ , \tag{4.1}$$

with $i=1,\ldots,4$ and $j=1,\ldots,4$. The coefficients mul-

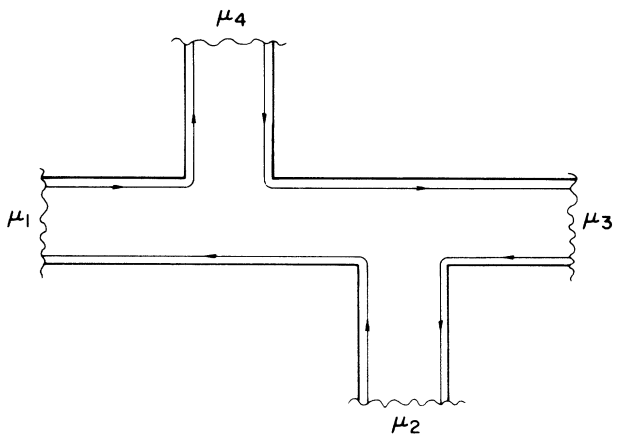

FIG. 11. Four-probe phase-coherent conductor with ideal contacts.

tiplying the chemical potentials in Eq. (4.1) form a matrix with the property that the elements of a column and of a row add up to zero. This is a consequence of current conservation. If current is fed in at contact m, withdrawn at contact n, and the voltage difference is measured between contacts k and l, the resistance is[8,10]

$$\mathcal{R}_{mn,kl}=(h/e^2)(T_{km}T_{ln}-T_{kn}T_{lm})/D \ . \tag{4.2}$$

Here, D is a subdeterminant of rank 3 of the matrix just discussed. The transmission and reflection probabilities in Eq. (4.1) obey the symmetry[8,10]

$$T_{ij}(\mathbf{B})=T_{ij}(-\mathbf{B}), \quad R_{ii}(\mathbf{B})=R_{ii}(-\mathbf{B}) \ , \tag{4.3}$$

if the Hamiltonian describing the sample is invariant under simultaneous reversal of momenta and magnetic field. Reference 8 shows that the determinant D is invariant under field reversal. Hence microreversibility [Eq. (4.3)] implies for Eq. (4.2) the reciprocity symmetry equation (1.1). Equations (4.1) and (4.2) have been useful for the discussion of the symmetry of the magnetoresistance[8,10,30] and the voltage and resistance fluctuations[49] of submicrometer conductors. The relationship of Eqs. (4.1)–(4.3) to the Kubo linear-response formalism is so far understood in some detail only for the case of weak magnetic fields. For a stimulating discussion of this point we refer to the paper by Stone and Szafer.[50] As mentioned in the Introduction, the relationship of Eqs. (4.1)–(4.3) to the quantum Hall effect has independently from us also been noted by Beenakker and van Houten[22] and Peeters.[24] Peeters,[24] in his discussion of the experiments of Roukes *et al.*,[24] considers Hall bars which are connected to the conductor via tunneling barriers.[10] He assumes from the outset a symmetry which is more special than that required by Eq. (1.1) or Eqs. (4.3). Below we present a general discussion of the role of contacts for the existence of the quantum Hall effect in phase-coherence conductors.

Let us start by considering the case of clean contacts. Figure 11 depicts the case of a magnetic field that points out of the plane of the paper. The transmission probabilities are $T_{41}=N$, $T_{34}=N$, $T_{23}=N$, and $T_{12}=N$. *All other transmission probabilities vanish.* The subdeterminant in Eq. (4.2) is $D=N^3$. Let us consider current flow from contact 1 to contact 3, and measure the voltage between contacts 2 and 4. The four-probe resistance $\mathcal{R}_{13,42}$ is a Hall-voltage measurement. Using the transmission probabilities as given above, we find $T_{41}T_{23}-T_{43}T_{21}=N^2$, and hence, the Hall voltage is

$$\mathcal{R}_H=\mathcal{R}_{13,42}=(h/e^2)(1/N) \ . \tag{4.4}$$

Suppose current flows from contact 1 to contact 4. The probes 2 and 3 are on the same side of the conductor with respect to the current source and drain and, hence, $\mathcal{R}_{14,23}$ is a "longitudinal" resistance. Now we have to consider $T_{21}T_{34}-T_{14}T_{31}$. Since T_{21} as well as T_{31} and T_{14} are zero, this expression is zero and, hence,

$$\mathcal{R}_L=\mathcal{R}_{14,23}=0 \ , \tag{4.5}$$

the "longitudinal" resistance, vanishes. Note that the outcome of all topologically equivalent resistance measurements is the same.

The conductor in Fig. 11 exhibits four sets of noninteracting edge states. There are a number of interesting sample topologies, characterized by ideal contacts, $R_{ii}=M-N$, which exhibit only three or two noninteracting sets of edge states. To consider briefly one such example, assume that only $N-K$ edge states emanating from contact 4 in Fig. 11 reach contact 3 and that K edge states emanating from contact 4 are deflected to contact 1. Similiarly, $N-K$ edge states emanating from contact 2 reach contact 1, whereas K edge states are deflected into contact 3. All N edge states from contact 1 reach contact 4 and all N ege states emanating from contact 3 reach contact 2. For $K<N$ the Hall resistance is quantized and given by $\mathcal{R}_{13,42}=(h/e^2)[1/(N-K)]$. Some edges of the conductor are equipotential lines and the corresponding longitudinal resistance vanishes, $\mathcal{R}_{14,23}=0$. On the other hand, the longitudinal resistance $\mathcal{R}_{12,43}$ is not zero, but quantized, and is given by

$$\mathcal{R}_{12,43}=(h/e^2)[K/N(N-K)] \ .$$

Since $K=N-(N-K)$ this resistance becomes

$$\mathcal{R}_{12,43}=(h/e^2)[1/(N-K)-1/N] \ ,$$

i.e., the difference between two two-terminal resistances for sample regions with $N-K$ and N edge states. A different derivation of this result has been given by van Houten *et al.*[23]

Next, we investigate deviations from the ideal situation discussed above. It can be shown that, if a single contact of the conductor of Fig. 11 is disordered, the Hall conductance is still quantized, and the "longitudinal" resistance is zero as for the conductor with ideal contacts. To make a connection with the discussion of Secs. II and III, and to show that contacts can be used to introduce inelastic scattering into the sample, we discuss the case of two disordered nonadjoining contacts. We show that we can use Eq. (4.1) to rederive Eqs. (2.25) and (2.26). The phase-coherent conductor of Fig. 11 with two ideal contacts is equivalent to the conductor of Fig. 9. Suppose contacts 1 and 3 are disordered and that contacts 2 and 4 are clean. The clean contacts are used to disrupt the phase of the edge states along the upper and lower edges of the sample. The two ideal contacts take the role of the phase-randomizing reservoirs μ_A and μ_B in Fig. 9. The matrices R_{ii} and T_{ij} have the following nonvanishing elements: Carriers incident at contact 1 are reflected with probability R_{11} and transmitted with probability T_{41} into contact 4. Since contact 4 is clean, carriers incident in contact 1 cannot reach contact 3 and hence cannot reach contact 2. Since the number of channels of the disordered contact is M, current conservation requires, $M=R_{11}+T_{41}$. We can introduce the abbreviation $T_1\equiv T_{41}$. Carriers incident on contact 2 can reach contact 1 with probability T_{12}. Both T_{13} and T_{14} are zero, and current conservation requires $R_{11}+T_{12}=M$. Thus $T_{12}=M-R_{11}=M-(M-T_{41})=T_{41}$ and we find $T_{12}=T_1$. Similar considerations determine the whole matrix of transmission and reflection probabilities. For clarity, we give all its elements,

$$R_{11}=M-T_1,\quad T_{12}=T_1,\quad T_{13}=0,\quad T_{14}=0\ , \tag{4.6a}$$

$$T_{21}=0,\quad R_{22}=M-N,\quad T_{23}\equiv T_2,\quad T_{24}\equiv R_2\ , \tag{4.6b}$$

$$T_{31}=0,\quad T_{32}=0,\quad R_{33}=M-T_2,\quad T_{34}=T_2\ , \tag{4.6c}$$

$$T_{41}=T_1,\quad T_{42}\equiv R_1,\quad T_{43}=0,\quad R_{44}=M-N\ . \tag{4.6d}$$

Note that T_1, T_2, R_1, and R_2 have been introduced as abbreviations and do not restrict the generality of these considerations. Using Eqs. (4.6) to evaluate Eqs. (4.2), and keeping in mind that the number of channels for all the contacts is $N_i=M$, yields

$$I_1=T_1\mu_1-T_1\mu_2\ , \tag{4.7a}$$

$$I_2=N\mu_2-T_2\mu_3-R_2\mu_4\ , \tag{4.7b}$$

$$I_3=T_2\mu_3-T_2\mu_4\ , \tag{4.7c}$$

$$I_4=-T_1\mu_1-R_1\mu_2+N\mu_4\ . \tag{4.7d}$$

The ideal contacts are voltage probes and thus $I_2=I_4=0$. This determines μ_2 and μ_4 and yields $\mu_4=\mu_A$ and $\mu_2=\mu_B$, given by Eqs. (2.25) and (2.26) with μ_2 replaced by μ_3. Using this in Eq. (4.7a) or (4.7c) yields the net current from contact 1 to contact 3 as given by Eq. (2.27) with μ_2 replaced by μ_3. This demonstrates that we could have obtained all the results presented in this paper by invoking only Eq. (4.1) (respectively, the generalization of this equation to an arbitrary number of contacts). The phase-randomizing reservoirs in Figs. 8(b), 9, and 10 can each be replaced by an ideal contact. Our demonstration stresses that an ideal contact acts like a phase-randomizing reservoir. Disordered contacts, on the other hand, lead only to a partial randomization of the phase.[13] Instead of randomizing the phase completely at one location, phase randomization can also be achieved through the action of many disordered contacts in series leading to spatially distributed inelastic scattering.

The phase-coherent conductor with two disordered contacts exhibits a quantized value for the Hall resistance [Eq. (4.4)] and exhibits a vanishing "longitudinal" resistance [Eq. (4.5)]. If two adjoining contacts are disordered this is typically not the case. Current injected through one of these contacts populates the edge states in a non-equilibrium fashion. If the adjoining contact is also disordered (exhibits internal reflection) it cannot equilibrate the edge states. As a consequence the Hall voltage is in general not quantized. The $N=1$ case is exceptional to the extent that evanescent waves can be neglected.[51] In the presence of a single edge state the possibility of phase coherent interference effects is greatly reduced. All four contacts need to be disordered (exhibit internal reflection) to produce deviations from the quantized Hall voltage. The consequences are the following: To observe the quantized Hall effect in a tiny sample constructed over a two-dimensional electron gas, with dimensions of an inelastic-scattering length, it is necessary to contact the sample in an ideal fashion. Elastic scattering at the contacts is detrimental to the quantum Hall effect. Carriers in such a small conductor are not subject to energy relaxation and the population of the edge states is not equilibrated. This causes deviations from exact quantization.

We have found that the Hall resistance is antisymmetric under field reversal whenever the resistance is quantized. This is due to the fact that certain transmission probabilities of the matrix T_{ij} are zero. If conditions for the breakdown of the quantum Hall effect are approached as in the experiments of Chang *et al.*,[18] simple examples discussed in Refs. 52 and 53 show that the measured Hall resistance is no longer antisymmetric. An additional feature of the four-terminal discussion of the Hall effect presented here is that it permits[10,53] negative "longitudinal" resistances. Negative-resistance fluctuations in the "longitudinal" resistance have been observed in Ref. 18. Clearly, these interesting phenomena deserve further experimental and theoretical attention.

Note added in proof. In Sec. II B and Fig. 6 we addressed the supression of the Aharonov-Bohm oscillations in high magnetic fields in ring structures. This effect has now been analyzed experimentally by Timp *et al.*[54] To observe Aharonov-Bohm effects, backscattering, either inside the conductor[21] or at the contacts, is essential.[55] In Sec. IV (see also Ref. 23) we discussed the quantization of longitudinal four-terminal resistances (unnumbered equations). This effect, closely related to the quantization of point contact resistances,[34] has been observed in multiterminal conductors by Washburn *et al.*[56] and Haug *et al.*[57] A linear response derivation of Eqs. (4.1) and (4.2) based on an extension of Refs. 38 and 50 has recently been given by Baranger and Stone.[58] The linear response kernel relating local current density and the local electric field also invokes states away from the Fermi energy. It is only the global transport coefficients relating chemical potentials of reservoirs and currents which are defined at the Fermi energy only. That the resistance formulas of Ref. 8 apply over the whole range of magnetic fields and invoke only states at the Fermi energy is very remarkable and will hopefully find further notice.

APPENDIX: LOCAL ELECTRIC POTENTIALS

The resistance equations (1.1) are determined by measuring *chemical* potentials at contacts.[8] These chemical potentials characterize an electron bath. The chemical potentials should be distinguished from the local electric potential $eU(x,y)$ which is defined at every point of the conductor.[10] There exists a potential $eU(x,y)$ which has the property that it matches the chemical potentials of the reservoirs and whose gradient determines the electric field, $\nabla U=-E(x,y)$. In the Landauer approach the incident current is specified as a function of the chemical potentials of the reservoirs. The potential U is determined by calculating the piled-up carriers in the presence of current flow, and by solving a Poisson equation. Consider a two-terminal conductor connected at the right and left to electron reservoirs at chemical potentials $\mu_1>\mu_2$. The extra charge density brought into the conductor due to the differing chemical potentials and due to a single quantum channel is

$$dn(x,y)=\frac{dn_j}{dE}(\mu_1-\mu_2)\,|\,\psi_j(x,y)\,|^2\,, \tag{A1}$$

where it is assumed that we know the wave function [Eqs. (2.12) and (2.13)] for the whole conductor. In Eq. (A1), $dn_j/dE=1/2\pi\hbar v_j$ is the density of states at the Fermi energy of the jth quantum channel in the perfect lead to the left. The total charge brought into the conductor due to N quantum channels is

$$dn=\frac{1}{h}(\mu_1-\mu_2)\sum_{j=1}^{j=N}\frac{1}{v_j}\,|\,\psi_j(x,y)\,|^2\,. \tag{A2}$$

Here we have used the density of states in the jth quantum channel $dn_j/dE=1/hv_j$. Let us use a Thomas-Fermi approximation to calculate self-consistent screening. The excess charge dn is screened by the charge density $dn_{\rm ind}$ induced by a local potential $eU(x,y)$,

$$dn_{\rm ind}=(eU-\mu_2)\frac{1}{h}\sum_{j=1}^{j=N}\frac{1}{v_j}(\,|\,\psi_j(x,y)\,|^2+|\,\psi_j'(x,y)\,|^2)\,. \tag{A3}$$

Here the wave functions with a prime describe carriers incident on the sample from the right-hand-side reservoir. Furthermore, we have assumed that the density of states for the quantum channels in the right- and left-hand perfect conductors are the same. [For high magnetic fields the upper and lower edge states have the same density of states only if the confining potential has a symmetry $V(y+a)=V(a-y)$, where a is the center position of the perfect conductor.] In Eq. (A3), $eU-\mu_2$ multiplies a local equilibrium density of states. We have assumed that the left- and right-hand perfect leads are identical (exhibit the same transverse quantum states). $U(x,y)$ is a solution of the equation[10]

$$\lambda^2\nabla^2 eU(x,y)+hv_0(dn-dn_{\rm ind})=0\,. \tag{A4}$$

Here we have introduced a screening length

$$\lambda=(\varepsilon_L/4\pi e^2)^{1/2}(dE/dn_0)^{1/2}$$

appropriate for the quantum channel $j=0$ with a density of states $dn_0/dE=1/hv_0$. Various perturbation techniques can be used to solve Eq. (A3) for the voltage U. For simplicity, we proceed as follows: Suppose that screening is very effective, i.e., that the screening length is short compared to the variation of the densities Δn and $\Delta n_{\rm ind}$. Then we can neglect the first term in Eq. (A4) and the resulting voltage[10,43] is given by Eq. (2.18). [The local potentials of Streda *et al.*[19] are obtained by considering Eq. (2.8) near the upper and lower edges of the sample. The wave functions, Eq. (2.12) and (2.13), in the perfect portions of the conductor are invoked. Interference terms[10] of the incident wave with the reflected waves are neglected in Ref. 19 as in Ref. 29. As long as the edge states are spatially well separated, this is justified.] Equations (A1)–(A4) are correct only if there are no localized states near the Fermi energy. If one wants to calculate $U(x,y)$ in a quantum Hall sample, away from the edges, then Eq. (A3) needs to be supplemented by the densities of the localized states. Such localized states act like an electron reservoir inside the sample and can affect the local potential U. We also note that Eq. (2.18) does not, in general, without additional conditions, satisfy the boundary condition required for eU; eU has to be equal to μ_1 in the left-hand reservoir and equal to μ_2 in the right-hand reservoir. In the calculation of eU, that can only be achieved if the contact resistances, the spreading out of the current in the reservoirs, is taken into account. This requires that the large density of states in the reservoirs is taken into account. A large density of states can be obtained by considering perfect leads which become much wider than the conductor as the reservoir is entered. It is necessary to consider contacts with a large number of channels M, as in Figs. 9 and 10, to obtain a self-consistent solution for the potential $eU(x,y)$.

ACKNOWLEDGMENTS

I am indebted to R. Landauer for urging me to complete this work. I also thank D. DiVincenzo, A. B. Fowler, Y. Imry T. Smith, J. R. Kirtley, S. Washburn, and A. D. Stone for comments on an earlier version of this manuscript.

[1]K. Von Klitzing, G. Dorda, and M. Pepper, Phys. Rev. Lett. **45**, 494 (1980).
[2]For reviews, see H. Aoki, Rep. Prog. Phys. **50**, 655 (1987); B. I. Halperin, Helv. Phys. Acta **56**, 75 (1983); D. R. Yennie, Rev. Mod. Phys. **59**, 781 (1987).
[3]R. B. Laughlin, Phys. Rev. B **23**, 5632 (1981).
[4]B. I. Halperin, Phys. Rev. B **25**, 2185 (1982).
[5]Y. Imry, J. Phys. C **16**, 3501 (1983).
[6]M. Büttiker, Y. Imry, and R. Landauer, Phys. Lett. **96A**, 365 (1983).
[7]Q. Niu and D. J. Thouless, Phys. Rev. B **35**, 2188 (1987).
[8]M. Büttiker, Phys. Rev. Lett. **57**, 1761 (1986).
[9]H. B. G. Casimir, Rev. Mod. Phys. **17**, 343 (1945).
[10]M. Büttiker, IBM J. Res. Dev. **32**, 317 (1988).
[11]Reciprocity theorems (in the absence of magnetic fields) have a long history: G. F. C. Searle, The Electrician **66**, 999 (1911).
[12]M. Büttiker, Phys. Rev. B **32**, 1846 (1985).
[13]M. Büttiker, Phys. Rev. B **33**, 3020 (1986); Bull. Am. Phys. Soc. **31**, 634 (1986); G. Timp, H. U. Baranger, P. de Vegvar, J. E. Cunningham, R. E. Howard, R. Behringer, and P. M. Mankiewich, Phys. Rev. Lett. **60**, 2081 (1988).
[14]J. R. Kirtley, Z. Schlesinger, T. H. Theis, F. P. Milliken, S. L. Wright, and L. F. Palmateer, Phys. Rev. B **34**, 1384 (1986); G. N. de Vegar, A. M. Chang, G. Timp, P. M. Mankiewich, J. E. Cunigham, B. Behringer, and R. E. Howard, *ibid.* **36**, 9366 (1987).
[15]K. K. Choi, D. C. Tsui, and S. C. Palmateer, Phys. Rev. B **33**, 8216 (1986).
[16]G. Timp, A. M. Chang, P. Mankiewich, R. Behringer, J. E.

Cunningham, T. Y. Chang, and R. E. Howard, Phys. Rev. Lett. **59**, 732 (1987); S. Datta, M. R. Melloch, S. Bandyopadhyay, R. Noren, M. Vaziri, M. Miller, and R. Reifenberger, *ibid.* **55**, 2344 (1985).

[17]M. L. Roukes, A. Scherer, S. J. Allen, Jr., H. G. Craighead, R. M. Ruthen, E. D. Beebe, and J. P. Harbison, Phys. Rev. Lett. **59**, 3011 (1987).

[18]A. M. Chang, G. Timp, T. Y. Chang, J. E. Cunningham, P. M. Mankiewich, R. E. Behringer, and R. E. Howard, Solid State Commun. **67**, 769 (1988).

[19]P. Streda, J. Kucera, and A. H. MacDonald, Phys. Rev. Lett. **59**, 1973 (1987).

[20]J. K. Jain and S. K. Kivelson, Phys. Rev. B **37**, 4276, (1988).

[21]J. K. Jain and S. A. Kivelson, Phys. Rev. Lett. **60**, 1542 (1988); J. K. Jain, *ibid.* **60**, 2074 (1988).

[22]C. W. J. Beenakker and H. van Houten, Phys. Rev. Lett. **60**, 2406 (1988).

[23]H. van Houten, C. W. J. Beenakker, P. H. M. van Loosdrecht, T. J. Thornton, H. Ahmed, M. Pepper, C. T. Foxon, and J. J. Harris, Phys. Rev. B **37**, 8534 (1988). The authors argue that the reduction of backscattering with increasing magnetic field explains the negative low-field magnetoresistance data of the experiments of Ref. 15.

[24]F. M. Peeters, Phys. Rev. Lett. **61**, 589 (1988).

[25]Y. Ono and T. Ohtsuki, Z. Phys. B **68**, 445 (1987).

[26]R. Johnston and L. Schweitzer, Z. Phys. B **70**, 25 (1988).

[27]R. Landauer, IBM J. Res. Dev. **1**, 233 (1957); R. Landauer, Philos. Mag. **21**, 863 (1970).

[28]R. Landauer, Z. Phys. B **68**, 217 (1987); IBM J. Res. Develop. **32**, 306 (1988).

[29]M. Büttiker, Y. Imry, R. Landauer, and S. Pinhas, Phys. Rev. B **31**, 6207 (1985).

[30]A. D. Benoit, S. Washburn, P. Umbach, R. B. Laibowitz, and R. A. Webb, Phys. Rev. Lett. **57**, 1765 (1986).

[31]L. L. Soethout, H. van Kempen, J. T. P. W. van der Maarseveen, P. A. Schroeder, and P. Wyder, J. Phys. F **17**, L129 (1987).

[32]E. K. Sichel, M. L. Knowles, and H. H. Sample, J. Phys. C **19**, 5695 (1986); E. K. Sichel, J. Appl. Phys. **61**, 1079 (1987).

[33]A. H. MacDonald and P. Streda, Phys. Rev. B **29**, 1616 (1984).

[34]B. J. van Wees, L. P. Kouwenhoven, H. van Houten, C. W. Beenaker, J. E. Mooij, C. T. Foxon, and J. J. Harris, Phys. Rev. B **38**, 3625 (1988); B. J. van Wees, H. van Houten, C. W. J. Beenakker, J. G. Williamson, L. P. Kouwenhoven, D. van der Marel, and C. T. Foxon, Phys. Rev. Lett. **60**, 848 (1988); D. A. Wharam, T. J. Thornton, R. Newbury, M. Pepper, H. Ahmed, J. E. F. Frost, D. G. Hasko, D. C. Peacock, D. A. Ritchie, and G. A. C. Jones, Phys. C **21**, 209 (1988).

[35]Y. Imry, *Physics of Mesoscopic Systems,* in Directions in Condensed Matter Physics, edited by G. Grinstein and G. Mazenko (World Scientific, Singapore, 1986), p. 101.

[36]Yu V. Sharvin, Zh. Eksp. Teor. Fiz. **48**, 984 (1965) [Sov. Phys.—JETP **21**, 665 (1965)].

[37]I. O. Kulik, A. N. Omel'yanchuk, and R. I. Shekhter, Fiz. Nisk. Temp. **3**, 1543 (1977) [Sov. J. Low. Temp. Phys. **3**, 740 (1977)]; A. G. M. Jansen, A. P. van Gelder, and P. Wyder, J. Phys. C **13**, 6073 (1980).

[38]D. S. Fisher and P. A. Lee, Phys. Rev. B **23**, 6851 (1981); E. N. Economou and C. M. Soukoulis, Phys. Rev. Lett. **46**, 618 (1981).

[39]T. Ohtsuki and Y. Ono, Solid State Commun. **65**, 403 (1988); B. Kramer, Y. Ono, and T. Othsuki, Surf. Sci. **196**, 127 (1988).

[40]S. Laux and F. Stern, Appl. Phys. Lett. **49**, 91 (1986).

[41]H. Levine, S. B. Libby, and A. M. M. Pruisken, Phys. Rev. Lett. **51**, 1915 (1983); D. E. Khmel'nitzkii, Pis'ma Zh. Teor. Fiz. **38**, 454 (1983) [JETP Lett. **38**, 552 (1983)].

[42]R. B. Laughlin, Phys. Rev. Lett. **52**, 2304 (1984).

[43]O. Entin-Wohlman, C. Hartzstein, and Y. Imry, Phys. Rev. B **34**, 921 (1986).

[44]Y. Gefen, Y. Imry, and M. Ya. Azbel, Phys. Rev. Lett. **52**, 129 (1984); M. Büttiker, Y. Imry, and M. Ya. Azbel, Phys. Rev. A **30**, 1982 (1984); R. A. Webb, S. Washburn, C. Umbach, and R. A. Laibowitz, Phys. Rev. Lett. **54**, 2696 (1985); A. D. Stone and Y. Imry, *ibid.* **56**, 189 (1986); R. Landauer and M. Büttiker, Phys. Rev. B **36**, 6255 (1987).

[45]R. E. Prange and R. Joynt, Phys. Rev. B **25**, 2943 (1982).

[46]D. J. Thouless, Phys. Rev. Lett. **39**, 1167 (1977).

[47]M. Büttiker, in *SQUIDS, Quantum Oscillations in Normal Metal Loops, Superconducting Quantum Intereference Devices and their Applications,* edited by H. D. Hahlbohm and H. Lübbig (de Gruyter, Berlin, 1985), p. 429.

[48]F. F. Fang and P. J. Stiles, Phys. Rev. B **27**, 6487 (1983); G. L. J. A. Rikken, J. A. M. M. van Haaren, W. van der Wel, A. P. van Gelder, H. van Kempen, P. Wyder, J. P. André, K. Ploog, and G. Weimann, *ibid.* **37**, 6181 (1988).

[49]A. D. Benoit, C. P. Umbach, R. B. Laibowitz, and R. A. Webb, Phys. Rev. Lett. **58**, 2343 (1987); W. J. Skoçpol, P. M. Mankiewich, R. E. Howard, L. D. Jackel, D. M. Tennant, and A. D. Stone, *ibid.* **58**, 2347 (1987); A. M. Chang, G. Timp, J. E. Cunningham, P. M. Mankiewich, R. E. Behringer, R. E. Howard, and H. U. Baranger, Phys. Rev. B **37**, 2745 (1988); M. Büttiker, *ibid.* **35**, 4123 (1987); S. Maekawa, Y. Isawa, and H. Ebisawa, J. Phys. Soc. Jpn. **56**, 25 (1987); H. U. Baranger, A. D. Stone, and D. P. DiVincenzo, Phys. Rev. B **37**, 6521 (1988); for additional references, see Ref. 10 and D. DiVincenzo and C. L. Kane, Phys. Rev. B **38**, 3006 (1988).

[50]A. D. Stone and A. Szafer, IBM J. Res. Dev. **32**, 384 (1988).

[51]C. W. J. Beenakker (private communication).

[52]M. Büttiker, Phys. Rev. Lett. (to be published).

[53]M. Büttiker, IBM Research Report No. RC 13951 (#62653) (unpublished).

[54]G. Timp, P. Mankiewich, P. de Vegvar, R. Behringer, J. E. Cunningham, R. E. Howard, and J. Jain (unpublished).

[55]U. Sivan and Y. Imry, Phys. Rev. Lett. **61**, 1001 (1988); U. Sivan, Y. Imry, and C. Hartzstein (unpublished).

[56]S. Washburn, A. B. Fowler, H. Schmid, and D. Kern (unpublished).

[57]R. J. Haug, A. H. MacDonald, P. Streda, and K. von Klitzing (unpublished).

[58]H. Branger and A. D. Stone (private communication).